Experiment on pulse heating and surface degradation of a copper cavity powered by powerful 30 GHz free electron maser

N. S. Ginzburg,[2] I. I. Golubev,[1] A. K. Kaminsky,[1] A. P. Kozlov,[1] S. V. Kuzikov,[2] E. A. Perelstein,[1] N. Yu. Peskov,[2] M. I. Petelin,[2] S. N. Sedykh,[1] A. P. Sergeev,[1] A. S. Sergeev,[2] A. A. Vikharev,[2] and N. I. Zaitsev[2]

[1]*Joint Institute for Nuclear Research, Dubna 141980, Russia*

[2]*Institute of Applied Physics, Russian Academy of Sciences, Nizhny Novgorod 603950, Russia*

(Received 13 January 2011; published 5 April 2011)

Experiments to investigate copper surface fatigue caused by pulsed rf radiation were carried out using the 30 GHz free electron maser. The copper surface of a special test cavity was exposed to 15–20 MW/150–200 ns rf pulses with a repetition rate of 1 Hz, providing a temperature rise of up to 250°C in each pulse. An electron microscope was used to study the copper surface both before and after exposure to 10^4–10^5 rf pulses. An examination of the copper microstructure and cracks which developed during the experiment was made. Dramatic degradation of the copper surface and causes of very frequent breakdown were observed when the total number of rf pulses reaches 6×10^4.

DOI: 10.1103/PhysRevSTAB.14.041002 PACS numbers: 52.59.−f, 29.20.Ej, 84.40.−x, 41.60.Cr

I. INTRODUCTION

The Compact Linear Collider (CLIC) project is currently undergoing intensive development. This collider is designed to achieve an acceleration gradient of ~100 MV/m using 12 GHz/200 ns pulses at a repetition rate of ~50 Hz. When operating at the design parameters, the temperature rise in the accelerating structures during the pulse would be ~50–60°C. The total number of the accelerating pulses is planned to be in the region of 2×10^{10} with a design lifetime of up to 20 years. One of the most dangerous threats to this project is repetitive rf pulsed heating of the copper accelerating structure, i.e., so-called thermal surface fatigue.

The fatigue effect was already known as parasitic phenomena arisen in high power, high repetition rate electron devices where the beam collector surface is heated by spent electrons [1]. Similar surface fatigue in the accelerating structures is a result of the mentioned above rf heating [2,3]. The physical cause of this effect is fast heating of the Ohmic skin layer caused by high-power rf radiation leading to thermal expansion of the hot upper metal layer which is resisted by the internal cold layers. This leads to mechanical stresses exceeding the strength of the metal. As a result, if the number of pulses is high enough, the metal surface becomes degraded, this could reduce the efficiency of the accelerating structures.

The first experimental study of the rf fatigue was performed at SLAC [4] using 11.4 GHz klystron. This experiment allowed the fatigue dependence on the temperature rise of the surface (which is determined by the rf pulse power and duration), the total number of pulses as well as the conductivity and mechanical properties of a metal to be concluded.

Further investigations were developed in two separate ways. Experimental data of the first type were obtained using modeling schemes (pulse heating by ultraviolet laser and cyclic ultrasound method) [5,6]. This method is rather extensive, however the scaling of these factors for practical predictions of a copper life time under intense rf-radiation power is still not clear. The second type of data related to direct rf heating experiments in special cavities [7,8] is more scant, because high-power experiments are rather expensive and complicated.

Experimental studies of the rf fatigue were intensified during the past few years. The reason is a solid experimental evidence that a high surface magnetic field, which is responsible for pulse heating, decreases the breakdown threshold of accelerating structures [9]. Recent experiments [10–12] have been demonstrated that the breakdown rate highly correlates with the pulse heating. These results clearly indicate that the pulse heating should be considered as a part of the breakdown phenomena. Nevertheless, an exact contribution of the magnetic rf field and the pulse heating into breakdown is not clear. Two mechanisms could be important. The first mechanism is based on the fact that local temperature rise at microinhomogeneities of the surface is essentially higher than the average temperature rise of the rest surface [13]. This explains an appearance and growth of the melted particles which due to metal evaporation could introduce trigger sources of the breakdown. The second mechanism does not totally exclude a possible stimulating role of the first mentioned effect, but exploits a hypothesis that electric field of the moderate level is enhanced at the surface small tips (or melted

particles) caused by the pulsed heating, and leads to the breakdown [14].

The present paper is devoted to the first experiments studying copper surface degradation at 30 GHz. Previous rf copper heating experiments were carried out at SLAC at the frequency of 11.4 GHz with a temperature rise of ~70–120°C during the pulse. These experiments demonstrated degradation of the copper surface after $\sim 10^6$–10^8 pulses [4,7,8]. Our studies were conducted to investigate copper fatigue at higher (~ 200°C) temperatures. The single-mode, high-efficiency free-electron maser (FEM) was constructed in cooperation between Joint Institute for Nuclear Research (JINR) (Dubna) and Institute of Applied Physics, Russian Academy of Sciences (IAP RAS) (Nizhny Novgorod) [15,16] and used as a source of the powerful rf pulses.

II. EXPERIMENTAL SETUP

A scheme of the experimental setup is shown in Fig. 1. The induction linac LIU-3000 (JINR) generates a 0.8 MeV/200 A/250 ns electron beam with a repetition rate of 1 Hz, which drives the FEM oscillator. A helical wiggler of 6 cm period pumps transverses velocity into the beam. The amplitude of the wiggler field was ~0.12 T, a reversed orientation guide magnetic field of ~0.15 T was used. A high-selectivity Bragg resonator with a step of phase of corrugation provides a feedback loop for the forward $TE_{1,1}$ wave and backward $TM_{1,1}$ wave in the vicinity of 30 GHz. The Bragg resonator was formed from two corrugated waveguide sections of 30 cm (upstream) and 15 cm (downstream) length (see [16] for more details).

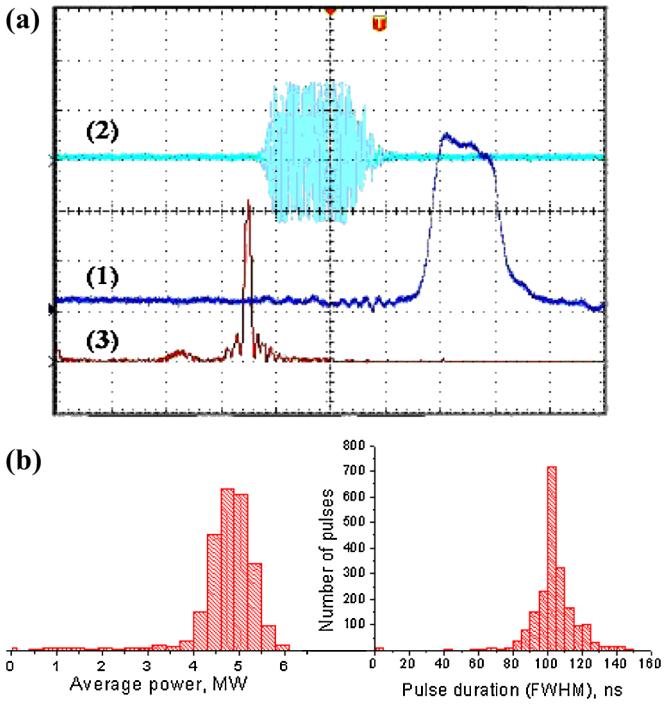

FIG. 2. (a) Typical oscilloscope traces of (1) rf pulse (100 ns/div), (2) heterodyne beat signal, and (3) frequency spectrum (50 MHz/div). (b) Statistic distributions of pulse duration and rf power after the test cavity in the series of 10^4 pulses.

In a recent series of experiments the FEM has generated 15–20 MW pulses of 150–200 ns duration. Calorimetric

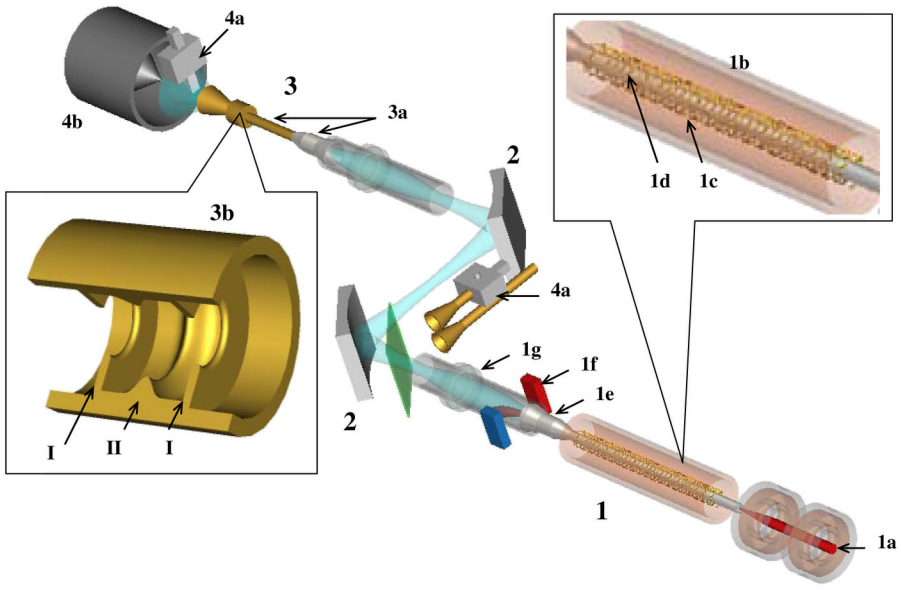

FIG. 1. Schematic diagram of the experimental setup: (1) 30-GHz JINR-IAP FEM (1a—electron beam, formed by linac; 1b—solenoid; 1c—helical wiggler; 1d—Bragg resonator; 1e—Gaussian beam mode converter, 1f—beam collector, 1g—output section based on Talbot effect). (2) Quasioptical transmission line. (3) Test resonator assembly (3a—input mode converters; 3b—test resonator itself: I—diaphragms, II—waistband); 4a rf detectors; 4b—calorimeter.

measurements indicate the energy content in each pulse amounted to 3 J. Typical oscilloscope traces of the rf pulse, heterodyne signal, and frequency spectrum are shown in Fig. 2(a). The oscillation frequency was measured as 29.92 GHz with a spectrum width of up to 6 MHz, close to the theoretical limit for a pulse of such duration. Acceptable stability of the radiation frequency, power, and pulse shape was achieved over a sequence of $\sim 10^5$ pulses [see Fig. 2(b)] [16].

To simulate the temperature regime of one of the CLIC project high-gradient accelerating structures, we used a high-Q test resonator which provided high intensity rf fields ($E \sim 200$ MV/m in the volume and $H \sim 1$ MA/m at the surface) when fed by the FEM pulses. The Fabry-Pérot–type test cavity was designed to operate at $TE_{0,1,1}$ mode. It was made from oxygen-free copper and had the form of two diaphragms with a profiled central section (''waistband'') in between (Fig. 3). The shape of the waistband was optimized to enhance the magnetic field in its center [Fig. 3(b)] in order to provide the required temperature rise during the rf pulse. Increasing the curvature of the waistband increased the maximum magnetic field and, hence, the peak heating temperature with an inevitable narrowing of the hot area. In different experimental series we could vary the temperature rise from 50° to 250°C. The test cavity operating mode was axially symmetrical and allowed study of the pulse heating effect in the absence of a normal to surface electric component [Fig. 3(c)], i.e., safely in the viewpoint of the rf breakdown. The highest surface heating occurred when the cavity Q factor was chosen to be in the range 1200–1500. A higher Q factor would decrease the spectral efficiency of the coupling of the feed radiation energy from the FEM to the test cavity. The resonant frequency of the cavity could be mechanically tuned to match the frequency of the FEM source.

The experimental setup included a two-mirror confocal transmission line and mode converters to transport the rf power from the FEM to the test cavity. ''Cold'' tests of all components of the experimental setup were carried out and demonstrated good agreement with the design parameters. The transmission efficiency of the FEM output power to the entrance and exit of the test cavity were measured as 80% and 25%–30%, respectively. A directional coupler was used to control both the incident and reflected powers.

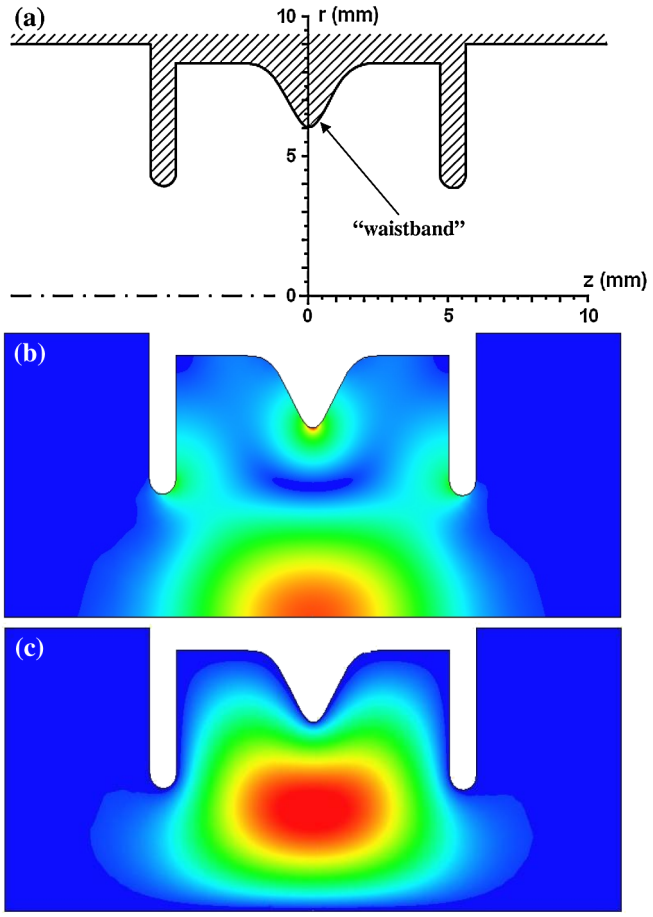

FIG. 3. (a) Scheme of the test cavity with the results of 3D simulation of (b) magnetic and (c) electric fields.

III. DEMONSTRATION OF BRAGG FEM OPERATION INTO A HIGH-Q LOAD

An important question which was solved at the preliminary stage of the conducted experiments is demonstration of the FEM ability to operate into a high-Q load. Even in the case of ideal matching the load frequency to the FEM operation frequency, strong reflections arise at the transient process when the rf pulse just comes into the load. These reflections could spoil the FEM generation regime. However, from the time-domain modeling [17] it was found that if the eigenfrequency of the load resonator coincides with the FEM operating frequency the load resonator becomes transparent and accumulation of the electromagnetic energy inside the resonator occurs (Fig. 4). The field amplitude inside the test resonator exceeds that in the incident wave by a factor of about $Q^{1/2}$. Detuning of the load-resonator frequency leads to strong

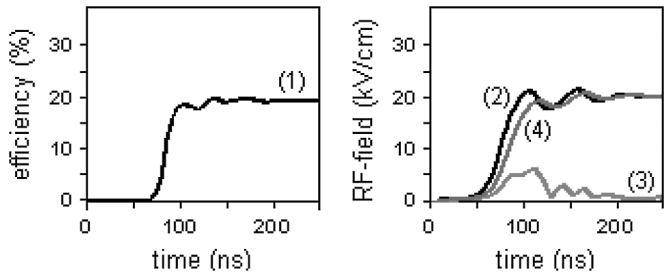

FIG. 4. Simulation of the FEM operation at a high-Q resonant load for parameters close to conditions of the JINR-IAP experiment with ideal matching between the load's and the radiation frequencies. Time dependence of (1) the FEM efficiency and wave beams (2) incident, (3) reflected, and (4) passed through the load.

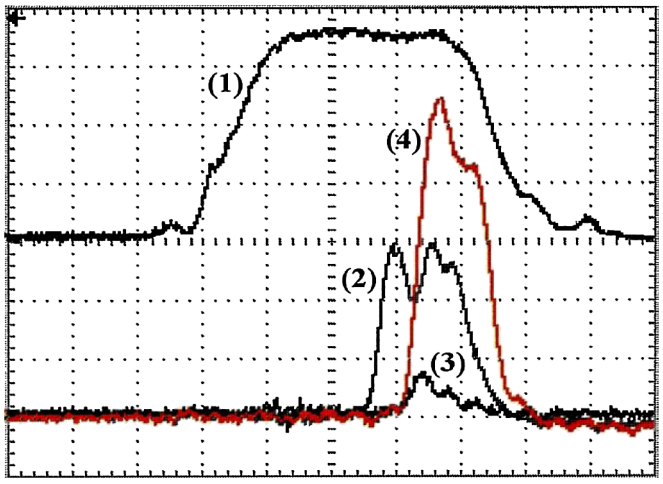

FIG. 5. FEM operating with the test resonator: oscilloscope traces of (1) beam current (60 A/div), (2) rf pulse at the FEM output (5 MW/div), (3) rf pulse reflected from the test resonator, and (4) rf pulse passed through the test resonator (0.5 MW/div); time scale is 100 ns/div.

reflections from this resonator which results in suppression of the FEM oscillations. At the same time, stability of the FEM operation can be improved when increasing (a) the time delay of the reflected from the load rf pulse and (b) the rf pulse losses in the transmission system.

During the experiments, stable operation of the FEM into a high-Q load was achieved (Fig. 5). In accordance with simulations, proper matching of the test cavity frequency to the FEM generation frequency allows low reflection from the cavity during the rf pulse, demonstrating the transparency of the test cavity and effective accumulation of the rf power within it. A 20% power attenuator was introduced to the transmission line to decrease the influence of the cavity reflection on the FEM operation. In addition, in order to delay the reflected signal relative to the FEM signal, the test cavity was placed at the distance of about 2 m from the FEM output (the delay time for the signal reflected from the test cavity was about 13 ns).

IV. RESULTS OF THE PULSE HEATING EXPERIMENTS

In the pulse heating experiments all calculations of the temperature rise at the waistband were based on calorimetric measurement of the rf power transmitted through the test cavity and measurement of the pulse envelope by means of a detector. These calculations were carried out after processing the recorded oscilloscope traces using the exact solution of the heat conductivity equation.

The first experiment was carried out with a test cavity providing a relatively low temperature rise ($\sim 50°$C) per rf pulse (waistband width $\sim$1 mm). These investigations have shown that fatigue was not observed for less than 10^5 pulses. This result agrees well with theoretical predictions [18] and previous experiments [4,7,8].

In the next experiments, the shape of the waistband was optimized in order to obtain a higher temperature rise per rf pulse, i.e., it was made more sharp, in order to strengthen the local magnetic field (Fig. 3). In this test cavity (with a 0.5 mm wide waistband), the temperature rise was increased to 220–250°C. To investigate fatigue damage after a number of pulses, the cavity surface was analyzed by means of optical and electronic microscopes. The initial copper surface has mainly small defects oriented along the waistband (see Fig. 6). These are grooves made by the cutting tool during the creation of the waistband shape, the surface roughness was about 0.8–1 μm.

Analysis of the microscope photographs showed different types of the surface damage after rf irradiation. During the first disassembly of the cavity (after $N_1 = 1.6 \times 10^4$ pulses), the effects were found only at the middle of the waistband and only in the form of protuberances of ten's microns size [Fig. 7(a)]. After the action of $N_2 = 3.2 \times 10^4$ pulses, we found that the number of surface damage sites increased and the area subject to damage expanded to either side of the waistband middle.

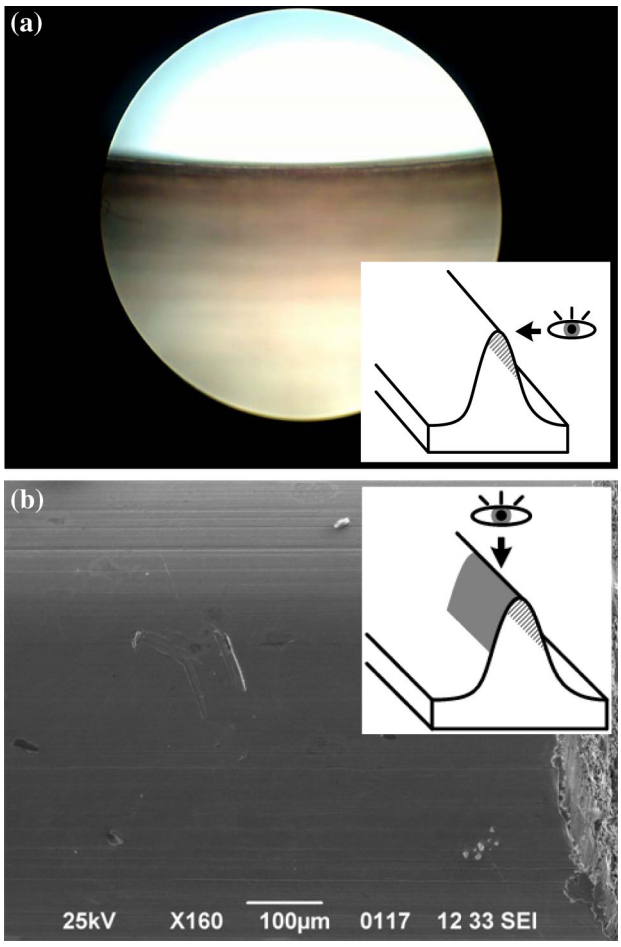

FIG. 6. Photographs of the central part of the waistband before FEM irradiation: (a) optical microscope and (b) electron microscope (magnification of 160).

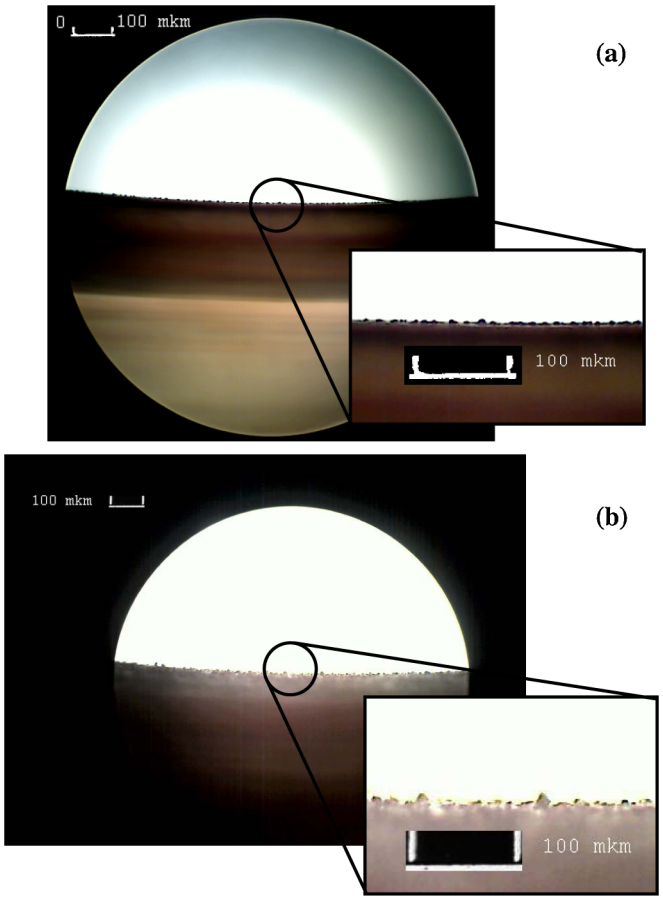

FIG. 7. Photographs (optical microscope) of the central part of the waistband after irradiation by (a) 1.6×10^4 and (b) 4.8×10^4 pulses (magnification of 160).

After $N_3 = 4.8 \times 10^4$ pulses, copper "drops" with the size ~10 microns appeared [Fig. 7(b)]. At this stage, the central section of the cavity with the waistband was slit up to several pieces which were examined more accurately using an electronic microscope (Fig. 8).

Next the experiment was repeated with a new cavity of the identical geometry. All disassemblies were performed after irradiation by the same number of pulses and coincide well with the experiments described above. The aim was to find the point when the surface damage would lead to significant changes of the cavity properties. After 6×10^4 pulses there was a significant decrease (about 4 times) in the signal from the calorimeter positioned after the test cavity accompanied by a shortening of the output rf pulse duration up to 40–60 ns. Simultaneously, the TV camera directed into the cavity registered rf breakdown, appearing at different azimuths of the waistband on practically every pulse. Note that the test cavity was operated in the $TE_{0,1}$ mode (which has no normal to the surface electric field), and breakdown was never observed except in the initial stages when the copper surface was being trained. The contaminants were pumped out of the vacuum vessel and as a result breakdown was not seen during the main stage of the experiment.

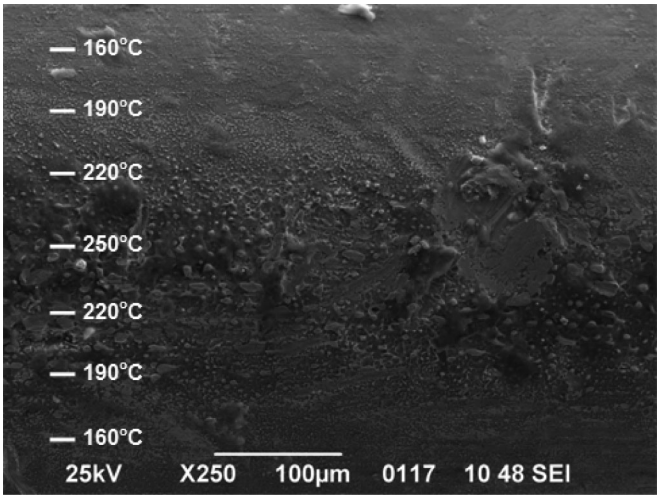

FIG. 8. Photograph (electron microscope) of the central part of the waistband after irradiation by 4.8×10^4 pulses (magnification of 250).

A photograph of the waistband surface after irradiation by the last series of pulses ($N_4 = 6 \times 10^4$ pulses), which was slit and made using an electronic microscope, is shown in Fig. 9. The calculated distribution of temperature (using calorimetric measurements of rf pulses passed through the test resonator) is indicated on the left-hand side. The large-scale photographs of three zones with temperature rises of about 250°C, 230°C, and 150°C are also shown in a column to the right of Fig. 9(a). It is seen that for a given number of pulses the boundary of surface degradation corresponds to the temperature rise of ~150–160°C. Near the middle of the waistband (temperature rise ~250°C) many "cracks" from tens to hundreds of microns depth were observed. These cracks were oriented along the copper crystal face [see Fig. 9(b)]. The disruption pattern was similar to that obtained in SLAC's experiments [4,7] where the temperature rise (60–100°C) was less than in our experiment but the total number of pulses (10^6–10^8) was more than in our experiment.

Our conclusion is that the pulse heating damage grows as the number of pulses increases and finally reaches a level that causes a breakdown (after 6×10^4 pulses). These conclusions are supported by examination of the exposed copper surface microstructure. One can see in Fig. 9(a) (right photograph at bottom) the after effects of a breakdown, i.e., copper melting. We suppose that these defects occur as a result of the deep fatigue growth which stimulates breakdown. However, the obtained results do not allow one to give full interpretation of the specific mechanisms of breakdown described in [13,14], which were mentioned in the Introduction. Possible reasons of the breakdown could be numerous melted particles observed in the experiment as well as the field enhancement at the

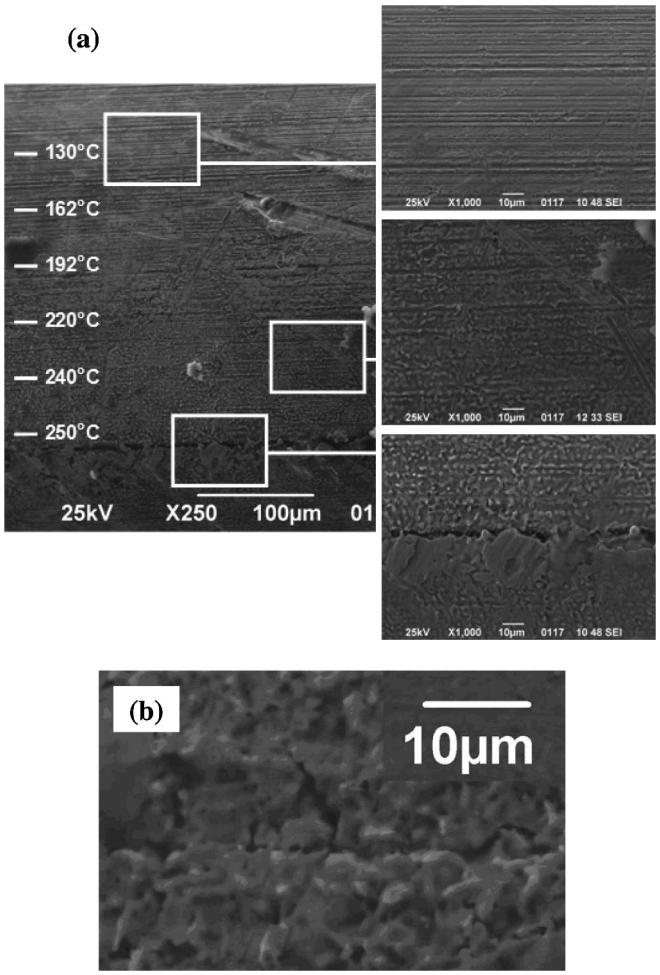

FIG. 9. (a) Photographs (electron microscope) of the central part of the waistband after irradiation by 6×10^4 pulses with magnification of 250 (left) and 1000 (right). (b) Central part of the waistband (different piece having temperature rise of ~250°C) with magnification of 3000.

sharp edges of the cracks. In the second case, a normal to surface electric field could be produced by a small admixture of spurious nonsymmetrical modes. This spurious radiation, estimated at the level less than 10%, was not sufficient to make the breakdown in the beginning of the experiment ($E \leq 30$ kV/cm at the surface), but, possibly, was enough after deep surface damage. Let us remind that in [14] the breakdown was regularly observed in the tested photonic band gap structure at only 140 kV/cm surface electric field, but 890 A/m magnetic field (temperature rise 85°C at most of 100 ns rf pulses). It was demonstrated [14] that the surface, located at the peak electric field, had no damage, but another surface, located at the peak magnetic field, had significant damages.

V. SUMMARY

In summary, the 30-GHz JINR-IAP FEM oscillator has been used for studies of surface pulse heating. The experiments show that a temperature rise of ~50°C per pulse does not degrade the properties of the test cavity for up to 10^5 pulses. Operation at a temperature rise of 200–250°C leads to dramatic degradation of the copper surface and causes very frequent breakdown when the total number of rf pulses reaches 6×10^4. Note, in conclusion, the degradation of metal surfaces under the action of multiple rf pulses is also an important effect to consider in the operation of powerful microwave devices [8].

ACKNOWLEDGMENTS

Authors would like to thank Dr. C. G. Whyte (University of Strathclyde, Glasgow, UK) for help in the work. This work is partially supported by the Russian Foundation for Basic Research and the Russian Federal Program "Scientific and Pedagogical Staff for Innovative Russia" for 2009–2013.

[1] V. F. Kovalenko, *Physics of Heat Transfer and Electrovacuum Devices* (Sovetskoe Radio, Moscow, 1975).
[2] O. A. Nezhevenko, in *Proceedings of the Particle Accelerator Conference, Vancouver, BC, Canada, 1997* (IEEE, New York, 1997), p. 3013.
[3] H. Braun, R. Corsini, J.-P. Delahaye, A. De Roeck, S. Doebert, G. Geschonke, A. Grudiev, C. Hauviller, B. Jeanneret, E. Jensen, T. Lefevre, Y. Papaphilippou, G. Riddone, L. Rinol, W. D. Schlatter, H. Schmickler, D. Schulte, I. Syratchev, M. Taborelli, F. Tecker, R. Tomas, S. Weisz, W. Wunsch, and A. Ferrari, CLIC-Note No. 764, 2008.
[4] D. P. Pritzkau and R. H. Siemann, Phys. Rev. ST Accel. Beams **5**, 112002 (2002).
[5] S. Calatroni, H. Nuepert, and M. Taborelli, in *Proceedings of the 9th European Particle Accelerator Conference, Lucerne, 2004* (EPS-AG, Lucerne, 2004), p. 557.
[6] S. Heikkinen, Doctoral thesis, Helsinki University of Technology, 2008.
[7] S. Tantawi, CLIC-2008 Workshop, CERN, Geneva, Switzerland, 2008.
[8] L. Laurent, U.S. High-Gradient Collaboration Workshop, Argonne, USA, 2009.
[9] V. A. Dolgashev, in *Proceedings of the 20th Particle Accelerator Conference, Portland, OR, 2003* (IEEE, New York, 2003), p. 1267.
[10] V. Dolgashev, S. Tantawi, Y. Higashi, and B. Spataro, Appl. Phys. Lett. **97**, 171501 (2010).
[11] F. Wang, Ch. Adolphsen, and Ch. Nantista, Phys. Rev. ST Accel. Beams **14**, 010401 (2011).
[12] A. A. Vikharev, N. S. Ginzburg, I. I. Golubev, Yu. Yu. Danilov, N. I. Zaitsev, A. K. Kaminsky, A. P. Kozlov, S. V. Kuzikov, E. A. Perelstein, N. Yu. Peskov, M. I. Petelin, S. N. Sedykh, A. P. Sergeev, and A. S. Sergeev, Tech. Phys. Lett. **37**, 102 (2011).
[13] G. S. Nusinovich, D. Kashyn, and T. M. Antonsen, Phys. Rev. ST Accel. Beams **12**, 101001 (2009).

[14] R. A. Marsh, M. A. Shapiro, R. J. Temkin, V. A. Dolgashev, L. L. Laurent, J. R. Lewandowski, A. D. Yeremian, and S. G. Tantawi, Phys. Rev. ST Accel. Beams **14**, 021301 (2011).

[15] N. S. Ginzburg, A. A. Kaminsky, A. K. Kaminsky, N. Yu. Peskov, S. N. Sedykh, A. P. Sergeev, and A. S. Sergeev, Phys. Rev. Lett. **84**, 3574 (2000).

[16] A. K. Kaminsky, E. A. Perelstein, S. N. Sedykh, N. S. Ginzburg, S. V. Kuzikov, N. Yu. Peskov, and A. S. Sergeev, Tech. Phys. Lett. **36**, 211 (2010).

[17] N. S. Ginzburg, A. K. Kaminsky, S. V. Kuzikov, E. A. Perelstein, N. Yu. Peskov, S. N. Sedykh, A. P. Sergeev, and A. S. Sergeev, Tech. Phys. **51**, 887 (2006).

[18] S. V. Kuzikov and M. E. Plotkin, Int. J. Infrared Millim. Waves **29**, 298 (2008).